Rapid Communication

Journal of PeptideScience

Received: 25 March 2010 Revised: 27 May 2010 Accepted: 1 June 2010 Published online in Wiley Interscience: 19 July 2010

(www.interscience.com) DOI 10.1002/psc.1271

A β-amino acid modified heptapeptide containing a designed recognition element disrupts fibrillization of the amyloid β-peptide

Valeria Castelletto,[a]* Ian W. Hamley,[a,b] Teck Lim,[c] Matias B. De Tullio[d] and Eduardo M. Castaño[d]

We study the complex formation of a peptide βAβAKLVFF, previously developed by our group, with Aβ(1–42) in aqueous solution. Circular dichroism spectroscopy is used to probe the interactions between βAβAKLVFF and Aβ(1–42), and to study the secondary structure of the species in solution. Thioflavin T fluorescence spectroscopy shows that the population of fibers is higher in βAβAKLVFF/Aβ(1–42) mixtures compared to pure Aβ(1–42) solutions. TEM and cryo-TEM demonstrate that co-incubation of βAβAKLVFF with Aβ(1–42) causes the formation of extended dense networks of branched fibrils, very different from the straight fibrils observed for Aβ(1–42) alone. Neurotoxicity assays show that although βAβAKLVFF alters the fibrillization of Aβ(1–42), it does not decrease the neurotoxicity, which suggests that toxic oligomeric Aβ(1–42) species are still present in the βAβAKLVFF/Aβ(1–42) mixtures. Our results show that our designed peptide binds to Aβ(1–42) and changes the amyloid fibril morphology. This is shown to not necessarily translate into reduced toxicity.

Supporting information may be found in the online version of this article

Keywords: amyloid beta peptide; beta-amino acid peptide; amyloid; fibril

Introduction

Amyloid diseases such as Alzheimer's and type II diabetes are becoming of increasing concern in societies in which people are enjoying longer and more affluent lives. Amyloid diseases are often believed to result from aggregation of misfolded proteins into β-sheet assemblies termed amyloid [1,2]. In the case of Alzheimer's, intense research activity has pointed to the role of the amyloid β (Aβ) peptide (which occurs in plasma and cerebrospinal fluid primarily in the forms Aβ(1–40) and Aβ(1–42) containing 40 or 42 residues, respectively) [3] in the disease pathology. It is presently thought that soluble oligomers of the Aβ peptide might be responsible for neurotoxicity [2,4,5]. The amyloid plaques observed *in vivo*, in brain sections from Alzheimer's sufferers, are large aggregates and are believed to be symptomatic of the condition, not the cause of it. Approaches to hinder the aggregation of oligomers (aggregation inhibitors) are actively being pursued as one possible route to the treatment of Alzheimer's [6–9]. Other major approaches include the development of γ-secretase enzyme inhibitors (β- and γ-secretase enzymes cleave the Aβ peptides from the amyloid precursor protein, APP) and the development of amyloid vaccines [6–9].

Inhibition of oligomer aggregation has been targeted via use of self-recognition elements (SREs). These are molecules based on fragments of the Aβ peptide, which are capable of binding to the corresponding sequence, but modified so as to disrupt β-sheet fibrillization (Scheme 1). Findeis *et al*. proved that compounds based on a core sequence of the Aβ peptide implicated in fibrillization, Aβ(16–20) (KLVFF), showed promise as SREs [10]. Murphy and coworkers have investigated the effect on Aβ aggregation of compounds based on KLVFF extended at the *C*-terminus by cationic or anionic residues to give KLVFFKKKKKK or KLVFFEEEE [11]. Molecules containing three or more lysines in the extension were found to be most effective [11,12]. Modified versions of these compounds have been used to examine the role of surface tension on the kinetics of aggregation of Aβ(1–40) [13]. The compounds contained modifications including charge, branching, D/L-isomer substitution and counterion type (motivated by the Hofmeister series) that influence the stabilization of the protein structure. Gordon *et al*. studied the *N*-methylated compound Aβ16–20m and showed that it inhibits fibrillization of Aβ(1–40) [14]. *N*-methylation of alternate residues disrupts β-sheet self-assembly due to the presentation on one face of the β-strand of residues incapable of adopting the usual hydrogen bonding pattern [14]. Doig and coworkers have followed this up and screened a number of *N*-methylated 'meptides' based

* *Correspondence to: Valeria Castelletto, Department of Chemistry, The University of Reading, Reading RG6 6AD, UK. E-mail: v.castelletto@reading.ac.uk*

a *Department of Chemistry, The University of Reading, Reading RG6 6AD, UK*

b *Diamond Light Source, Chilton, Didcot, Oxfordshire OX11 0DE, UK*

c *Department of Materials, University of Oxford, Parks Road, Oxford OX1 3PH, UK*

d *Fundación Instituto Leloir-Instituto de Investigaciones Bioquímicas de Buenos Aires, Consejo Nacional de Investigaciones Científicas y Técnicas (CONICET), Patricias Argentinas 435, Buenos Aires C1405BWE, Argentina*

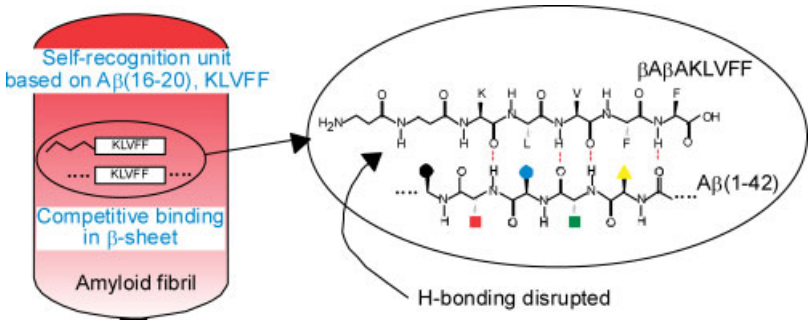

Scheme 1. Self-recognition element based on βAβAKLVFF.

originally on the same sequence, but with all D-amino acids and with modifications of the termini and incorporation of branched residues in certain positions, which are promising as SREs toward targeted aggregation inhibitor agents, and which also contain elements to improve their pharmacokinetics [15]. Doig has also reviewed other promising compounds [7], Austen *et al*. have developed compounds based on KLVFF but with terminal modifications to aid solubility and showed that these were effective inhibitors of toxicity using human neuroblastoma cells [16]. Mihara *et al*. have shown that even dipeptides LF and CF can form mixed fibrils with small amounts of Aβ(1–42), hence 'capturing' the peptide [17]. The binding of β-alanine and GABA-modified peptide fragments to amyloid fibrils formed by α-synuclein, Aβ(1–40) and amylin has recently been examined [18]. The binding sequence was based on self-recognition element V^{77}AQKTV^{82} of the full-length peptide and shorter sequences therefrom.

Alternative techniques have been developed to reduce neuronal damage due to exposition to Aβ(1–40) and Aβ(1–42). For example, a recent paper [19] shows that the alkaloid galantamine (Reminil®) is able to inhibit the action of the enzyme acetylcholinesterase, improving the memory and recognition of individuals with diseased brains.

In this article, we study the binding of an SRE based to a core sequence of the Aβ peptide (Scheme 1). We have prepared a variant of this peptide, extended by two β-alanine residues at the *N*-terminus to give βAβAKLVFF [20]. β-Amino acids have a propensity to drive peptides to form α-helical structures [21–23] and in addition are resistant to proteolysis (the sequence KLVFF, being based on conventional amino acids, is not resistant to endoproteases). This peptide is of potential interest as an SRE that may disrupt β-sheet fibrillization of Aβ(1–42) because the βA residues cannot be integrated into the hydrogen-bonding pattern of the other residues (Scheme 1). We show here that this rational design strategy leads to a molecule that can bind to Aβ(1–42) and change the fibril morphology.

Here, we report on the study of the complexation of βAβAKLVFF with Aβ(1–42) in aqueous solutions of Tris–HCl 20 mM/NaCl 50 mM buffer, pH 7.4 (Tris buffer). Circular dichroism (CD) was used to study the secondary structure and binding effects in solutions containing Aβ(1–42)/βAβAKLVFF mixtures. Thioflavin T (ThT) binding, assayed by fluorescence spectroscopy was used to probe peptide fibril formation. The self-assembled structures obtained in Aβ(1–42)/βAβAKLVFF mixtures were investigated using a combination of transmission electron microscopy (TEM) and cryo-TEM. Neurotoxicity assays were performed on Aβ(1–42)/βAβAKLVFF mixtures in order to assess the utility of these samples as therapeutic agents.

Table 1. Compositions of samples investigated

Name	Sample composition	Molar ratio
Aβ : βP 1 : 0	50 μM Aβ(1–42)	1 : 0
Aβ : βP 1 : 0.5	50 μM Aβ(1–42) + 25 μM βAβAKLVFF	1 : 0.5
Aβ : βP 1 : 1	50 μM Aβ(1–42) + 50 μM βAβAKLVFF	1 : 1
Aβ : βP 1 : 1.5	50 μM Aβ(1–42) + 75 μM βAβAKLVFF	1 : 1.5

Experimental

Materials

βAβAKLVFF (H-β^2Ala-β^2Ala-Lys-Leu-Val-Phe-Phe-OH) was custom synthesized by CS Bio Company (Menlo Park, CA) as a TFA salt. Purity was 98% based on HPLC (TFA in water/acetonitrile gradient) M_w found 795.27 by electrospray MS. Amyloid Aβ(1–42) (H-Asp-Ala-Glu-Phe-Arg-His-Asp-Ser-Gly-Tyr-Glu-Val-His-His-Gln-Lys-Leu-Val-Phe-Phe-Ala-Glu-Asp-Val-Gly-Ser-Asn-Lys-Gly-Ala-Ile-Ile-Gly-Leu-Met-Val-Gly-Gly-Val-Val-Ile-Ala-OH) was purchased from American Peptide Inc. (Sunnyvale, USA). Purity was 95.8% based on RP-HPLC chromatography, M_w found 4514.1 by electrospray MS.

In order to prevent any pre-aggregation, Aβ(1–42) was first dissolved in hexafluoroisopropanol (HFIP) at a final concentration of 1 mg ml^{-1} [24–26]. HFIP was then evaporated under a slow stream of N_2. Aβ(1–42) was re-suspended in Tris buffer. When necessary, Aβ(1–42) was re-suspended in Tris buffer with βAβAKLVFF peptide. Aβ(1–42)/βAβAKLVFF solutions and samples containing pure Aβ(1–42) were then incubated at 20 °C without agitation. We studied samples containing 50 μM Aβ(1–42) or mixtures of 50 μM Aβ(1–42) with βAβAKLVFF in different molar ratios = $1:\frac{[\beta A\beta AKLVFF]}{[A\beta(1-42)]}$ = 1 : 0.5, 1 : 1 and 1 : 1.5 ([] = molar concentration). The samples were therefore labeled Aβ : βP 1 : 0, Aβ : βP 1 : 0.5, Aβ : βP 1 : 1 and Aβ : βP 1 : 1.5 (where βP stands βAβAKLVFF β-alanine peptide), according to the compositions detailed in Table 1.

Circular Dichroism

The CD spectra were recorded at 20 °C on a Chirascan spectropolarimeter (Applied Photophysics, UK). Solutions Aβ : βP 1 : 0, Aβ : βP 1 : 0.5, Aβ : βP 1 : 1 and Aβ : βP 1 : 1.5 were incubated for 4 days and then studied by CD. Control βAβAKLVFF solutions were also studied by CD. Peptide solutions were loaded into 0.1 mm quartz

Journal of PeptideScience

cells or 1 mm quartz bottles. The CD data were measured using 1-s acquisition time per point and 1-nm step. Each CD spectrum was averaged over repeated replicate scans. The post-acquisition smoothing tool from Chirascan software was used to remove random noise elements from the averaged spectra. A residual plot was generated for each curve in order to verify whether or not the spectrum has been distorted during the smoothing process. The CD signal from the Tris solvent was subtracted from the CD data of the peptide solutions. Following background correction, the CD data were normalized to molar mean residue ellipticity.

Thioflavin T Fluorescence Spectroscopy

Spectra were recorded at 20 °C on a Perkin Elementar Luminescence spectrometer LS50B with samples in a 0.5-cm-thick quartz cell. A solution containing 150 μM ThT in Tris buffer was prepared and used as a solvent to prepare Aβ : βP 1 : 0, Aβ : βP 1 : 0.5, Aβ : βP 1 : 1 and Aβ : βP 1 : 1.5 solutions. These solutions were then incubated for 4 days. After this period of incubation, the concentration of Aβ : βP 1 : 0, Aβ : βP 1 : 0.5, Aβ : βP 1 : 1 and Aβ : βP 1 : 1.5 solutions containing ThT was reduced by a factor 6 through dilution in Tris buffer. The fluorescence of these samples was then measured using $\lambda_{ex} = 440$ nm. The fluorescence data were corrected for Tris buffer background.

Transmission Electron Microscope

TEM experiments were performed using a Philips CM20 transmission electron microscope operated at 80 kV while high-resolution TEM (HR-TEM) was done using a JEOL JEM-4000 microscope operated at 200 kV. Aβ : βP 1 : 0, Aβ : βP 1 : 0.5, Aβ : βP 1 : 1 and Aβ : βP 1 : 1.5 solutions were incubated for 4 days before being studied by TEM. Droplets of the solutions were placed on Cu grids coated with a carbon film (Agar Scientific, UK), stained with uranyl acetate (1 wt%) (Agar Scientific, UK) and dried.

Cryo-TEM

Aβ : βP 1 : 0 and Aβ : βP 1 : 1.5 solutions were studied by Cryo-TEM after 7 days of incubation. Experiments were performed using a Jeol 2100 microscope at Unilever Corporate Research (Colworth, UK). The sample was placed on a holey carbon 400 mesh Cu TEM grid in a controlled humidity (85 ± 3% RH) chamber at 22 ± 2 °C. The sample on the grid was then blotted using a Gatan Cp3 cryoplunge system to create a thin film. Afterward, the grid with the sample was quickly vitrified by immersion in liquid ethane [27] and carefully transferred under a liquid-nitrogen environment to the microscope.

Primary Neuronal Cultures

The hippocampus of Wistar rat embryos (E17) was dissected free of meninges and digested with 0.25% trypsin at 37 °C for 25 min. After washing with Neurobasal medium containing 10% fetal bovine serum supplemented with B-27 and N-2 (GIBCO) and penicillin/streptomycin, tissue was homogenized with a fire-polished Pasteur pipette to obtain a single-cell suspension. Cells were seeded at 30 000 cells/well in P96 plates for MTT assays. The plates were coated with poly-lysine (0.25 mg ml^{-1}) before use. After 3 h of incubation under 5% CO_2 at 37 °C to permit cell attachment, the medium was replaced with the same medium but without serum. Neuronal purity of the cultures was 90–95%. After

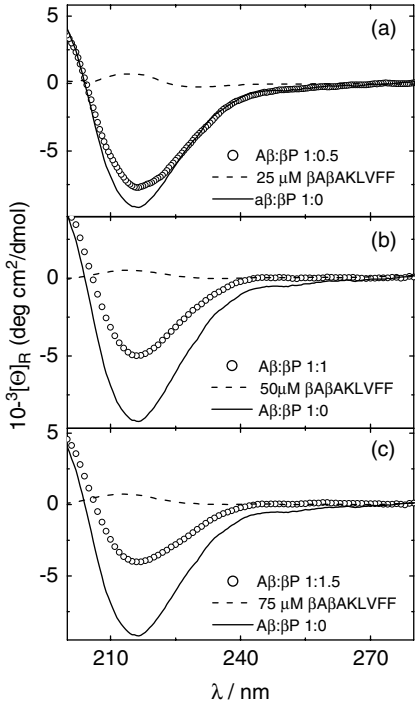

Figure 1. CD spectra for Aβ : βP 1 : 0 and (a) 25 μM βAβAKLVFF and Aβ : βP 1 : 0.5; (b) 50 μM βAβAKLVFF and Aβ : βP 1 : 1 and (c) 75 μM βAβAKLVFF and Aβ : βP 1 : 1.5 solutions.

14 days of initiation, the cultures were subjected to treatments as described below in the Neurotoxicity Assays section. Protocols for the handling of the rats used for these cultures followed the guidelines of the National Institute for Neurological Disorders and Stroke and were reviewed and approved by the Committee for the Care and Use of Laboratory Animals of the Fundación Instituto Leloir.

Neurotoxicity Assays

Neuronal damage was assessed by MTT assays. In this way, quantitative estimation of cellular death was assessed through the reduction of yellow MTT (3-(4,5-dimethylthiazolyl-2-yl)-2,5-diphenyltetrazolium bromide) to purple formazan by mitochondria of living cells (MTT assay, Sigma Aldrich).

Samples in Table 1 were incubated for 4 days, diluted 1 : 5 in culture medium and exposed to neurons (treated as described in the Primary Neuronal Cultures section) for 20 h, before undertaking MTT assays. Then, 15 ml of 0.5 wt% MTT substrate in PBS buffer was added to each P96 plate well and incubated for 45 min at 37 °C. In order to stop the MTT reaction and consequent formazan solubilization, 50 ml of 10% Triton X-100 (0.1 M HCl) was added to each P96 plate well and left at room temperature in the dark for 2 h. Finally, formazan absorbance was measured at 570 nm with a microtiter plate reader 550 (Bio-Rad). Hydrogen peroxide (H_2O_2) at 0.05% was used as a positive control for toxicity.

Results and Discussion

Figure 1 shows the CD results obtained for Aβ : βP 1 : 0, Aβ : βP 1 : 0.5, Aβ : βP 1 : 1 and Aβ : βP 1 : 1.5 solutions (Table 1) together with the CD measured for the control solutions containing 25, 50 and 75 μM βAβAKLVFF.

The CD spectra for Aβ : βP 1 : 0, Aβ : βP 1 : 0.5, Aβ : βP 1 : 1 and Aβ : βP 1 : 1.5 solutions present a negative band centered 216 nm, characteristic of a β-sheet structure [28]. The intensity of the negative band at 216 nm decreases upon increasing the content of βAβAKLVFF in the sample. It is possible to ascribe this behavior to an interaction between Aβ(1–42) and βAβAKLVFF, since the spectra in Figure 1 confirm binding between both peptides (as discussed below).

The CD data for Aβ : βP 1 : 0 solution in Figure 1 can be compared with the previous data in the literature, although it can be affected by the incubation time and the origin of Aβ(1–42). In the previous work, the aging behavior of a 44 μM Aβ(1–42) sample in water (pH 6) was monitored using CD [29]. At time $t = 0$, the spectrum was characterized by a broad minimum at ~215 nm characteristic of a β-sheet conformation. After 7 days, this minimum underwent a red shift to 226 nm, attributed to the appearance of distorted (helically twisted) β-strands [29]. A similar result was found by CD for the aging of 116 μM Aβ(1–42) solutions in 0.1 M Tris–HCl (pH 7.4) pre-incubated at 37 °C [30]. In that case, the broad minimum shifted from 200 to 219 cm^{-1}, when the pre-incubation time increased from 0 to 31 days [30].

The CD spectra for the control samples 25–75 μM βAβAKLVFF present a maximum at ~214 nm and a minimum at ~232 nm. According to our previous work [31–33], and in agreement with reports on CD for phenylalanine oligopeptides [34], a positive Cotton effect at ~214 nm may be associated with the $\pi-\pi^*$ interactions of phenylalanine units [35]. The CD spectra indicate that βAβAKLVFF is not aggregated into an ordered secondary structure under the conditions investigated.

The CD data in Figure 1 clearly shows that the features for Aβ : βP 1 : 0.5, Aβ : βP 1 : 1 and Aβ : βP 1 : 1.5 solutions do not resemble those observed for βAβAKLVFF solutions, but those measured for Aβ : βP 1 : 0 solution. Therefore, it is necessary to address the question of whether Aβ(1–42) and βAβAKLVFF indeed form a binary complex. In order to investigate the complexation of the two peptides, the linear addition of the CD spectrum for the 50 μM Aβ(1–42) solution and the CD spectrum for 25 μM βAβAKLVFF was calculated, providing a calculated spectrum for Aβ : βP 1 : 0.5 solution (Table 1, Figure 2a). A similar procedure was followed to calculate the CD spectra for Aβ : βP 1 : 1 (Figure 2b) and Aβ : βP 1 : 1.5 solutions (Figure 2c). Figure 2 compares the calculated and measured CD spectra for the mixtures. It is clear from Figure 2 that the measured CD spectra for the mixtures does not correspond to a linear addition of the spectra for the two peptides, indicating that βAβAKLVFF interacts with Aβ(1–42) to form a complex, i.e. that binding occurs which influences the chiral structure of βAβAKLVFF and/or Aβ(1–42) molecules.

Amyloid formation in the βAβAKLVFF/Aβ(1–42) mixtures was further studied by ThT fluorescence, a dye staining method commonly used as a diagnostic for amyloid formation [36,37].

The fluorescence of the pure ThT sample was characterized by a single broad peak centred at 482 nm (Figure S1). The intensity of the fluorescence of the ThT peak was enhanced for solutions containing Aβ(1–42) and βAβAKLVFF. Figure 3 shows the dependence of I/I_o on $\frac{[\beta A\beta AKLVFF]}{[A\beta(1-42)]}$ (I = intensity of the ThT fluorescence peak for samples containing Aβ(1–42), I_o = the intensity of the fluorescence peak for a pure ThT solution). It is evident from Figure 3 that Aβ(1–42) on its own gives rise to enhanced ThT fluorescence, denoting the formation of peptide fibrils. The ThT fluorescence is enhanced even more through the addition of βAβAKLVFF to samples containing Aβ(1–42). The

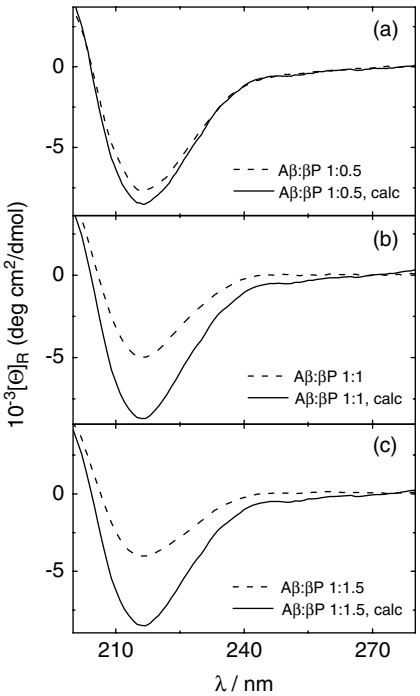

Figure 2. (- - - -) Measured vs (———) calculated CD spectrum for (a) Aβ : βP 1 : 0.5, (b) Aβ : βP 1 : 1 and (c) Aβ : βP 1 : 1.5 solutions.

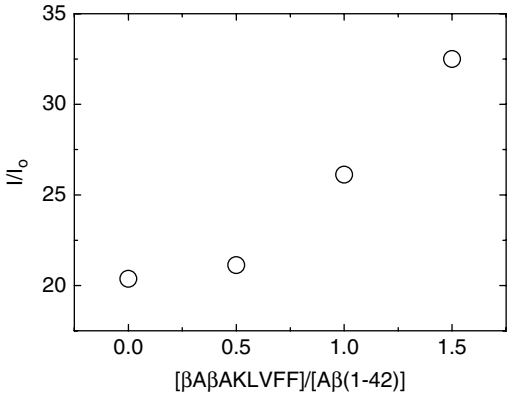

Figure 3. Intensity ratio of ThT fluorescence for samples containing Aβ(1–42) and βAβAKLVFF (I) normalized by the intensity of the pure ThT solution (I_o), plotted as a function of [βAβAKLVFF]/[Aβ(1–42)].

data in Figure 3 supports the idea that βAβAKLVFF is binding increasingly to Aβ(1–42) upon increasing molar ratio.

ThT fluorescence experiments also provided additional information about the formation of Aβ(1–42)/βAβAKLVFF complexes. The ThT fluorescence for the control samples containing only βAβAKLVFF was characterized by the ThT emission peak at 482 and an additional peak at 560 nm (Figure S1). The emission peak at 560 nm is absent for ThT on its own and in ThT solutions containing Aβ(1–42) (results not shown). An emission peak at ~560 nm was previously observed by us for FFKLVFF stained with congo red [32] and ThT/FFFF-PEG_{3000} solutions [33]. A similar peak has been reported for other amphiphilic molecules comprising aromatic moieties conjugated to PEG chains [38]. We have previously associated the emission peak at 560 nm to aggregates which arise from stacking of aromatic moieties [39]. These aggregates are present at

Journal of PeptideScience

very low peptide concentration, and they precede the formation of β-sheets fibrils observed at high peptide concentrations.

The absence of the 560 nm peak emission for Aβ(1–42)/βAβAKLVFF/ThT solutions, together with the Aβ(1–42)/βAβAKLVFF binding observed in Figure 2, provides information about the structure of solutions with molar ratio = 1 : 0.5–1 : 1.5. It is evident from those results that the formation of Aβ(1–42)/βAβAKLVFF complexes is the preferred state relative to βAβAKLVFF self-assembly for Aβ(1–42)/βAβAKLVFF mixtures.

The self-assembly of βAβAKLVFF, Aβ(1–42) and the mixtures was further studied by TEM and cryo-TEM (Figure S2). There are a few earlier reports on the use of cryo-TEM to study the self-assembly of Aβ(1–42) or related peptides [40]. It has also been used to examine the fibrillization of KLVFF and related peptides [20,41,42]. The vitrification process in cryo-TEM should ensure that the aggregates present in the aqueous solution are 'trapped' and directly imaged *in situ*.

HR-TEM micrographs for dried films obtained from Aβ : βP 1 : 0, Aβ : βP 1 : 0.5 and Aβ : βP 1 : 1 solutions are shown in Figure 4a, Figure 4b,c and Figure 4d,e, respectively (TEM data obtained for Aβ : βP 1 : 1.5 is shown in Figure S3).

HR-TEM images reveal the formation of straight 8.2 $\pm$ 0.9-nm-thick fibers for Aβ : βP 1 : 0 solution (Figure 4a). The Aβ : βP 1 : 0 solution presented highly polydisperse long fibers, whose full extended length could not be determined by TEM. However, we could estimate from our TEM images that Aβ : βP 1 : 0 solution fibers can attain a lower limit average length of 755 $\pm$ 445 nm.

The fibres in Figure 4a are similar to those reported in the literature. Straight 6–9 nm diameter fibrils, were observed by TEM on a dried film obtained from a 10 µM Aβ(1–42) solution in PBS (pH 7.4), incubated for 2 days at 22 °C [43]. Fibrils with 9–14 nm diameter have been reported from TEM on a dried film obtained from a 100 µM Aβ(1–42) solution in PBS (pH 7.4), incubated for 4 days at 37 °C [15]. Standard features of amyloid fibers, 10 nm in width, have also been reported from TEM on dried films obtained from a 230 µM Aβ(1–42) solution in PBS (pH 7.4) incubated for 2 days at 37 °C [44].

HR-TEM data for Aβ : βP 1 : 0.5 solution shows that the co-incubation of Aβ(1–42) with βAβAKLVFF results in the formation of dense clumps of short fibrils (Figure 4b and c). These short fibers are not straight, as observed for Aβ(1–42) alone, but curvy. The fibril clumps are formed by 8.2 $\pm$ 0.5 nm thick short curvy fibrils. HR-TEM data for Aβ : βP 1 : 0.5 solution also shows the existence of numerous very short isolated fibers 8.8 $\pm$ 0.8 nm thick, with a highly polydisperse length of 38.4 $\pm$ 14 nm and globules with diameter of 7.9 $\pm$ 1.1 nm. A few long isolated straight fibers coexist with the curvy short fibers, fiber clumps and globules.

We interpret the globules observed for Aβ : βP 1 : 0.5 solution as being the spherical oligomeric aggregates previously noted for Aβ(1–42) in the literature. Earlier work on such structures is reviewed elsewhere [4,5,45,46]. Typically annular assemblies of synthetic Aβ are donut-like structures with an outer diameter of 8–12 nm and an inner diameter of 2–2.5 nm [5]. Smaller oligomeric species have also been observed for synthetic Aβ and are known as Aβ-derived diffusible ligands (ADDLs), they are globules with diameter 5–6 nm that have been shown to exhibit neurotoxicity [4,47]. Short protofibrils ranging from monomers to pentamers, as well as smaller nuclei, were reported for Aβ42 oligomers on the basis of light scattering, TEM and SDS-PAGE experiments [3]. Conventional TEM also indicates 5 nm diameter objects for Aβ(1–42) oligomers, these being ascribed to pentameric/hexameric 'paranuclei' [48]. A recent study using mass spectrometry with molecular modeling indicates that the cross-section of oligomeric aggregates ranges from 12.5 nm^2 (dimers) to 42 nm^2 (dodecamers) [49,50].

HR-TEM results for the Aβ : βP 1 : 1 solution (Figure 4d and e) and TEM results for Aβ : βP 1 : 1.5 solution (Figure S3) were qualitatively similar to those found for the Aβ : βP 1 : 0.5 solution in Figure 4b and c.

The results obtained from the cryo-TEM studies on Aβ : βP 1 : 0 and Aβ : βP 1 : 1.5 solutions (Figure S2) are consistent with the results presented in Figure 4. The cryo-TEM data obtained for Aβ : βP 1 : 0 shows a coexistence of open networks of short fibers and globules (Figure S2a). The globules range in size between 9 and 4 nm, whereas Aβ (1–42) fibers are 8.3 $\pm$ 0.2 nm thick. Cryo-TEM reveals that the addition of βAβAKLVFF to Aβ(1–42), with molar ratio = 1 : 1.5, results in an extended network of 7.6 $\pm$ 1.0 nm thick short curvy fibrils (Figure S2b).

According to the TEM and cryo-TEM results discussed, globular-oligomeric species can be observed for samples containing pure Aβ(1–42) or mixed with βAβAKLVFF. Indeed, TEM results suggest that the main effect resulting from the addition of βAβAKLVFF to Aβ(1–42) solutions consists in the formation of short curvy fibrils which can be found isolated or self-assembled into clumps. This result was confirmed by cryo-TEM, as the extended networks of curvy fibrils visualized *in situ* by cryo-TEM seem to correspond to the clumps of fibers measured by TEM. The curvy fibrils found for molar ratio = 1 : 0.5–1 : 1.5 are shorter than the straight fibers observed for Aβ(1–42) solution, and the TEM and cryo-TEM images show that they are deposited considerably more densely than in the absence of βAβAKLVFF, which can explain the increase in ThT fluorescence observed in Figure 3.

In their study of the binding of peptide fragments modified with β-alanine or GABA, Madine *et al*. [18] noted that the co-incubation of the β-alanine peptide fragments with the full peptides (α-synuclein or amylin) led in some cases to the disruption of fibrils and consequent formation of dense fibrillar aggregates, similar to those shown in Figure 4.

It is evident from TEM results that βAβAKLVFF is able to disrupt amyloid fibrils to produce new species consisting of short curvy fibers, which might alter the toxicity of the system. It is therefore necessary to establish whether βAβAKLVFF stabilizes additional Aβ(1–42) toxic species, increasing the intrinsic neurotoxicity of self-assembled Aβ(1–42).

The neurotoxicity of Aβ(1–42) and Aβ(1–42)/βAβAKLVFF mixtures was assessed against primary rat neuronal cultures. This particular cellular system was chosen because it has proven very sensitive to the effect of Aβ (1–42) oligomers or protofibrils [51,52].

MTT assays were performed to evaluate the cytoxicity induced by Aβ : βP 1 : 0, Aβ : βP 1 : 0.5, Aβ : βP 1 : 1 and Aβ : βP 1 : 1.5 solutions. The corresponding results are displayed in Figure 5. MTT assays were also undertaken on neurons treated only with Tris buffer and on neurons treated with βAβAKLVFF solutions with concentrations equal to those used for Aβ : βP 1 : 0.5, Aβ : βP 1 : 1 and Aβ : βP 1 : 1.5 solutions (Figure 5).

A significant reduction in the MTT assay (~21% lower than control) from cell homogenates was measured for neurons treated with Aβ(1–42) solution (Figure 5). In addition, MTT assays show that Aβ(1–42)/βAβAKLVFF mixtures presented a toxicity similar to that obtained for Aβ(1–42) alone (Figure 5), as the difference obtained between Aβ(1–42) alone and Aβ(1–42)/βAβAKLVFF mixtures is within the error provided by the standard deviation of the results. These results indicate that, at least at the concentrations

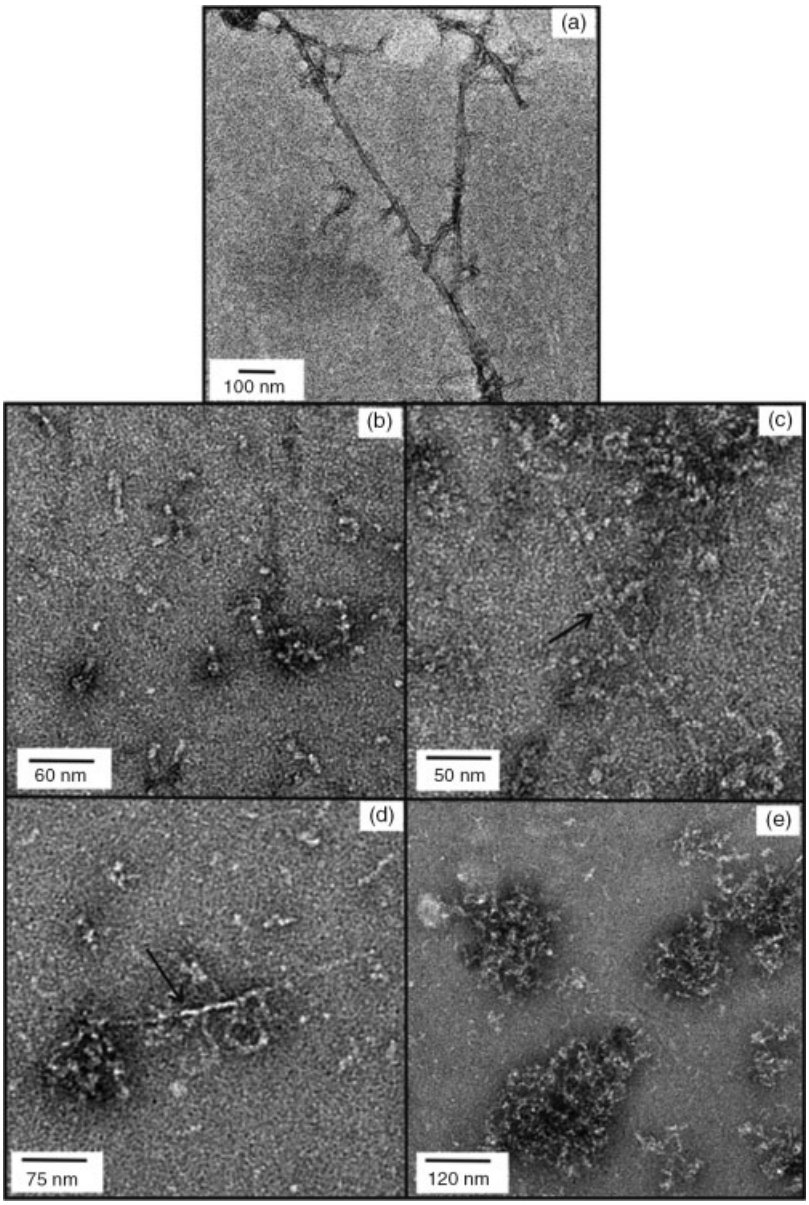

Figure 4. HR-TEM images for dried films obtained from (a) Aβ : βP 1 : 0, (b and c) Aβ : βP 1 : 0.5 (d and e) Aβ : βP 1 : 1 solutions. The arrows in (c and d) point to straight longer fibers.

studied here (up to 75 μM), βAβAKLVFF does not counteract the cytoxicity of Aβ(1–42). However, the peptide does not enhance cytoxicity.

Conclusions

In this work, we obtained clear evidence for the binding of βAβAKLVFF to amyloid β peptide Aβ(1–42). The CD data points to the interaction of the two peptides, as the CD spectra observed for the mixtures cannot be represented by the addition of the CD spectra obtained for the individual compounds. Fluorescence experiments using the chromophore ThT indicate enhanced fibrillization in the presence of βAβAKLVFF and Aβ(1–42) compared to Aβ(1–42) alone. TEM and cryo-TEM demonstrate clear differences upon addition of βAβAKLVFF. Most importantly, the co-incubation of βAβAKLVFF with Aβ(1–42) causes pronounced changes in fibril morphology compared to the straight fibrils observed for Aβ(1–42) alone and leads to the formation of extended dense networks of short chains.

Here, we show that although the complexation of βAβAKLVFF with Aβ(1–42) disrupts Aβ(1–42) fibrillization, it does not noticeably change the toxicity level of Aβ(1–42) alone. Toxic Aβ(1–42) species are still present in the βAβAKLVFF/Aβ(1–42) mixtures. These initial results have been very valuable in screening studies, and related compounds which can reduce the cytoxicity of Aβ(1–42) are under development. Our results show that binding of a peptide to Aβ(1–42) with a concomitant change in fibril morphology does not *per se* demonstrate suitability toward therapeutic applications.

This statement does not apply in general to all β-amino acid peptides. Related studies [18] have shown that peptides containing β-amino acids can function as oligomer aggregation inhibitors and still appear promising for possible therapeutic applications. It will

Journal of PeptideScience

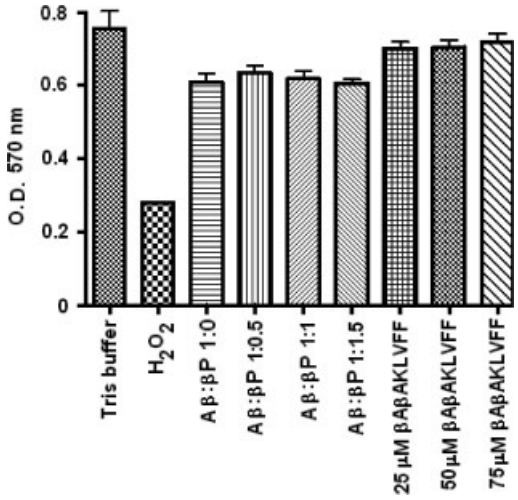

Figure 5. Quantitative MTT assay on Aβ:βP 1:0, Aβ:βP 1:0.5, Aβ:βP 1:1, Aβ:βP 1:1.5 solutions, together with the corresponding MTT control experiments (neurons treated with Tris buffer and βAβAKLVFF solutions).

be therefore interesting to incorporate additional β-amino acids to further improve resistance to proteolysis as βAβAKLVFF is expected to be stable against *N*-terminal aminopeptidases, but not against *C*-terminal carboxypeptidases or endopeptidases [2].

Acknowledgements

We would like to acknowledge Prof. J. Gibbins (School of Biological Sciences, University of Reading) for providing the facilities for the fluorescence experiments. The EPSRC is thanked for funding the access to the TEM instruments in Oxford Materials under the Materials Equipment Access scheme, grant reference: EP/F01919X/1. Steve Furzeland and Derek Atkins are thanked for assistance with cryo-TEM at Unilever (Colworth, UK). This work was supported by EPSRC grants EP/F048114/1, EP/G030952/1 and EP/G026203/1 to IWH. We thank the reviewers for helpful comments which have significantly improved the final presentation of this manuscript.

Supporting information

Supporting information may be found in the online version of this article.

References

1 Chiti F, Dobson CM. Protein misfolding, functional amyloid, and human disease. *Annu. Rev. Biochem.* 2006; **75**: 333–366.
2 Hamley IW. Peptide fibrillization. *Angew. Chem. Int. Edit.* 2007; **46**: 8128–8147.
3 Walsh DM, Lomakin A, Benedek GB, Condron MM, Teplow DB. The oligomerization of amyloid β-protein begins intracellularly in cells derived from human brain. *J. Biol. Chem.* 1997; **272**: 22364–22372.
4 Irvine GB, El-Agnaf OMA, Shankar GM, Walsh DM. Protein aggregation in the brain: the molecular basis for Alzheimer's and Parkinson's diseases. *Mol. Med.* 2008; **14**: 451–464.
5 Selkoe DJ. Soluble oligomers of the amyloid beta-protein impair synaptic plasticity and behavior. *Behav. Brain Res.* 2008; **192**: 106–113.
6 Roberson ED, Mucke L. 100 years and counting: prospects for defeating Alzheimer's disease. *Science* 2006; **314**: 781–784.
7 Doig AJ. Peptide inhibitors of beta-amyloid aggregation. *Curr. Opin. Drug Discov.* 2007; **10**: 533–539.
8 Melnikova I. Therapies for Alzheimer's disease. *Nat. Rev. Drug Discov.* 2007; **6**: 341–342.
9 Holtzman DM. Alzheimer's disease – moving towards a vaccine. *Nature* 2008; **454**: 418–420.
10 Findeis MA, Musso GM, Arico-Muendel CC, Benjamin HW, Hundal AM, Lee JJ, Chin J, Kelley M, Wakefield J, Hayward NJ, Molineaux SM. Modified-peptide inhibitors of amyloid beta-peptide polymerization. *Biochemistry* 1999; **38**: 6791–6800.
11 Lowe TL, Strzelec A, Kiessling LL, Murphy RM. Structure–function relationships for inhibitors of beta-amyloid toxicity containing the recognition sequence KLVFF. *Biochemistry* 2001; **40**: 7882–7889.
12 Pallitto MM, Ghanta J, Heinzelman P, Kiessling LL, Murphy RM. Recognition sequence design for peptidyl modulators of β-amyloid aggregation and toxicity. *Biochemistry* 1999; **38**: 3570–3578.
13 Gibson TJ, Murphy RM. Design of peptidyl compounds that affect beta-amyloid aggregation: importance of surface tension and contex. *Biochemistry* 2005; **44**: 8898–8907.
14 Gordon DJ, Tappe R, Meredith SC. Design and characterization of a membrane permeable *N*-methyl amino acid-containing peptide that inhibuits Aβ 1–40 fibrillogenesis. *J. Pept. Res.* 2002; **60**: 37–55.
15 Kokkoni N, Stott K, Amijee H, Mason JM, Doig AJ. N-methylated peptide inhibitors of beta-amyloid aggregation and toxicity. Optimization of the inhibitor structure. *Biochemistry* 2006; **45**: 9906–9918.
16 Austen BM, Paleologou KE, Ali SAE, Qureshi MM, Allsop D, El-Agnaf OMA. Designing peptide inhibitors for oligomerization and toxicity of Alzheimer's beta-amyloid peptide. *Biochemistry* 2008; **47**: 1984–1992.
17 Sato J, Takahashi T, Oshima H, Matsumura S, Mihara H. Design of peptides that form amyloid-like fibrils capturing amyloid beta 1–42 peptides. *Chem. Eur. J.* 2007; **13**: 7745–7752.
18 Madine J, Wang X, Brown DR, Middleton DA. Evaluation of beta-alanine- and GABA-substituted peptides as inhibitors of disease-linked protein aggregation. *ChemBioChem* 2009; **10**: 1982–1987.
19 Matharu B, Gibson G, Parsons R, Huckerby TN, Moore SA, Cooper LJ, Millichamp R, Allsop D, Austen B. Galantamine inhibits beta-amyloid aggregation and cytotoxicity. *J. Neurol. Sci.* 2009; **280**: 49–58.
20 Castelletto V, Hamley IW, Hule RA, Pochan DJ. Helical-ribbon formation by a beta-amino acid modified amyloid beta-peptide fragment. *Angew. Chem. Int. Edit.* 2009; **48**: 2317–2320.
21 Seebach D, Matthews JL. Beta-peptides: a surprise at every turn. *Chem. Commun.* 1997; 2015–2022.
22 Seebach D, Overhand M, Kuhnle FNM, Martinoni B, Oberer L, Hommel U, Widmer W. Beta-peptides: synthesis by Arndt-Eistert homologation with concomitant peptide coupling. Structure determination by NMR and CD spectroscopy and by X-ray crystallography. Helical secondary structure of a beta-hexapeptide in solution and its stability towards pepsin. *Helv. Chim. Acta* 1996; **79**: 913–941.
23 Cheng RP, Gellman SH, DeGrado WF. Beta-peptides: from structure to function. *Chem. Rev.* 2001; **101**: 3219–3232.
24 Bose PP, Chatterjee U, Nerelius C, Govender T, Norstrom T, Gogoll A, Sandegren A, Gothelid E, Johansson J, Arvidsson PI. Poly-N-methylated amyloid beta-peptide (A beta) C-terminal fragments reduce a beta toxicity in vitro and in Drosophila melanogaster. *J. Med. Chem.* 2009; **52**: 8002–8009.
25 Anker JN, Hall WP, Lambert MP, Velasco PT, Mrksich M, Klein WL, Van Duyne RP. Detection and identification of bioanalytes with high resolution LSPR spectroscopy and MALDI mass spectrometry. *J. Phys. Chem. C* 2009; **113**: 5891–5894.
26 Chromy BA, Nowak RJ, Lambert MP, Viola KL, Chang L, Velasco PT, Jones BW, Fernandez SJ, Lacor PN, Horowitz P, Finch CE, Krafft GA, Klein WL. Self-assembly of A beta(1–42) into globular neurotoxins. *Biochemistry* 2003; **42**: 12749–12760.
27 Talmon Y. Transmission electron microscopy of complex fluids: the state of the art. *Ber Bunsen-Ges. Phys. Chem.* 1996; **3**: 364–372.
28 Kelly SM, Jess TJ, Price NC. How to study proteins by circular dichroism. *Biochim. Biophys. Acta* 2005; **1751**: 119–139.
29 Laczko I, Vass E, Soos K, Fulop L, Zarandi M, Penke B. Aggregation of Ab(1–42) in the presence of short peptides: conformational studies. *J. Pept. Sci.* 2008; **14**: 731–741.
30 Sian AK, Frears ER, El-Agnaf OMA, Patel BP, Manca MF, Siligardi G, Hussain R, Austen BM. Oligomerization of beta-amyloid of the Alzheimer's and the Dutch-cerebral-haemorrhage types. *Biochem. J.* 2000; **349**: 299–308.

31 Hamley IW, Krysmann MJ, Kelarakis A, Castelletto V, Noirez L, Hule RA, Pochan DJ. Nematic and columnar ordering of a PEG-peptide conjugate in aqueous solution. *Chem. Eur. J.* 2008; **14**: 11369–11375.
32 Krysmann MJ, Castelletto V, Hamley IW. Fibrillisation of hydrophobically modified amyloid peptide fragments in an organic solvent. *Soft Matter* 2007; **2**: 1401–1406.
33 Castelletto V, Hamley IW. Self assembly of a model amphiphilic phenylalanine peptide/polyethylene glycol block copolymer in aqueous solution. *Biophys. Chem.* 2009; **141**: 169–174.
34 Peggion E, Palumbo M, Bonora GM, Toniolo C. *Bioorg. Chem.* 1974; **3**: 125.
35 Gupta M, Bagaria A, Mishra A, Mathur P, Basu A, Ramakumar S, Chauhan VS. Self-assembly of a dipeptide-containing conformationally restricted dehydrophenylalanine residue to form ordered nanotubes. *Adv. Mat.* 2007; **19**: 858.
36 LeVine H. Thiflavine-T interaction with synthetic Alzheimers-disease beta-amyloid peptides – detection of amyloid aggregation in solution. *Protein Sci.* 1993; **2**: 404–410.
37 Nilsson MR. Techniques to study amyloid fibril formation in vitro. *Methods* 2004; **34**: 151–160.
38 Lee E, Huang Z, Ryu J-H, Lee M. Rigid-flexible block molecules based on a laterally extended aromatic segment: hierarchical self-assembly into single fibers, flat ribbons and twisted ribbons. *Chem. Eur. J.* 2008; **14**: 6957–6966.
39 Smith AM, Williams RJ, Tang C, Coppo P, Collins RF, Turner ML, Saiani A, Ulijn RV. Fmoc-diphenylalanine self assembles to a hydrogel via a novel architecture based on $\pi-\pi$ interlocked β-sheets. *Adv. Mat.* 2008; **20**: 37–41.
40 Bohrmann B, Adrian M, Dubochet J, Kuner P, Muller F, Huber W, Nordstedt C, Dobeli H. Self-assembly of beta-amyloid 42 is retarded by small molecular ligands at the stage of structural intermediates. *J. Struct. Biol.* 2000; **130**: 232–246.
41 Krysmann MJ, Castelletto V, Kelarakis A, Hamley IW, Hule RA, Pochan DJ. Self-assembly and hydrogelation of an amyloid peptide fragment. *Biochemistry* 2008; **47**: 4597–4605.
42 Castelletto V, Hamley IW, Harris PJF, Olsson U, Spencer N. Influence of the solvent on the self-assembly of a modified amyloid beta peptide fragment. I. Morphological investigation. *J. Phys. Chem. B* 2009; **13**: 9978–9987.
43 Fezoui Y, Teplow DB. Kinetic studies of amyloid beta-protein fibril assembly – differential effects of alpha-helix stabilization. *J. Biol. Chem.* 2002; **227**: 36948–36954.
44 Wood SJ, Maleeff B, Hart T, Wetzel R. Physical, morphological and functional differences between pH 5.8 and 7.4 aggregates of the Alzheimer's amyloid peptide aβ. *J. Mol. Biol.* 1996; **256**: 870–877.
45 Teplow DB. Structural and kinetic features of amyloid beta-protein fibrillogenesis. *Amyloid* 1998; **5**: 121–142.
46 Caughey B, Lansbury PT. Protofibrils, pores, fibrils, and neurodegeneration: separating the responsible protein aggregates from the innocent bystanders. *Annu. Rev. Neurosci.* 2003; **26**: 267–269.
47 Lambert MP, Barlow AK, Chromy BA, Edwards C, Freed R, Liosatos M, Morgan TE, Rozovsky I, Trommer B, Viola KL, Wals P, Zhang C, Finch CE, Krafft GA, Klein WL. Diffusible, nonfibrillar ligands derived from A beta(1–42) are potent central nervous system neurotoxins. *Proc. Natl. Acad. Sci. U.S.A.* 1998; **95**: 6448–6453.
48 Bitan G, Kirkitadze MD, Lomakin A, Vollers SS, Benedek GB, Teplow DB. Amyloid beta-protein (A beta) assembly: a beta 40 and A beta 42 oligomerize through distinct pathways. *Proc. Natl. Acad. Sci. U.S.A.* 2003; **100**: 330–335.
49 Bernstein SL, Dupuis NF, Lazo ND, Wyttenbach T, Condron MM, Bitan G, Teplow DB, Shea J-E, Ruotolo BT, Robinson CV, Bowers MT. Amyloid-beta protein oligomerization and the importance of tetramers and dodecamers in the aetiology of Alzheimer's disease. *Nat. Chem.* 2009; **1**: 326–331.
50 Yu L, Edalji R, Harlan JE, Holzman TF, Lopez AP, Labkovsky B, Hillen H, Barghorn S, Ebert U, Richardson PL, Miesbauer L, Solomon L, Bartley D, Walter K, Johnson RW, Hajduk PJ, Olejniczak ET. Structural characterization of a soluble amyloid beta-peptide oligomer. *Biochemistry* 2009; **48**: 1870–1877.
51 Ward RV, Jennings KH, Jepras R, Neville W, Owen DE, Hawkins J, Christie G, Davis JB, George A, Karran EH, Howlett DR. Fractionation and characterization of oligomeric, protofibrillar and fibrillar forms of beta-amyloid peptide. *Biochem. J.* 2000; **348**: 137–144.
52 Giuffrida ML, Caraci F, Pignataro B, Cataldo S, De Bona P, Bruno V, Molinaro G, Pappalardo G, Messina A, Palmigiano A, Garozzo D, Nicoletti F, Rizzarelli E, Copani A. Beta-amyloid monomers are neuroprotective. *J. Neurosci.* 2009; **34**: 10582–10587.

